
Direct evidence for the existence of energy-based texture mechanisms

Nicolaas Prins

Department of Psychology, University of Mississippi, Oxford, MS 38677, USA;
e-mail: nprins@olemiss.edu

Frederick A A Kingdom

McGill Vision Research, McGill University, 687 Pine Avenue West, H4-14, Montréal, Québec H3A 1A1, Canada

Received 20 January 2005, in revised form 11 August 2005; published online 21 July 2006

Abstract. Two classes of models have been proposed to explain how the visual system processes texture modulations. In ‘feature models’, abstract representations of the featural properties of local texture regions (eg orientation, spatial frequency, contrast) are first generated, after which differences in individual feature properties across space are detected. In ‘energy models’, on the other hand, differences across space in the response energies of linear simple-cell-like filters are detected. This model thus processes the existing differences between texture regions directly without generating a full representation of the individual texture regions. We provide here direct evidence for the existence of the second, energy model, using an adaptation paradigm in conjunction with textures simultaneously modulated in two dimensions—orientation and spatial frequency. We found that the mechanism that processed the conjoint modulation was tuned to orientations and spatial frequencies that could not be predicted by any feature model, but which were precisely predicted by the energy model.

1 Introduction

Spatial variations in texture characteristics such as local orientation and spatial frequency provide the observer with important information about the shape of a textured object or surface (Cutting and Millard 1984; Frisby and Buckley 1992; Knill 1998, 2001; Li and Zaidi 2000). For example, depth variations in a textured 3-D surface translate into orientation and spatial-frequency modulations in the 2-D retinal image. Much is known about the mechanisms that are sensitive to the orientation and spatial frequency of localized image features. Hubel and Wiesel (1962) mapped the receptive fields of cells in cat primary visual cortex and showed that many cells displayed orientation selectivity, being responsive only to bars presented at certain orientations. Later, Campbell et al (1969) determined that cortical cells are also narrowly tuned for spatial frequency. The local characteristics of orientation and spatial frequency are thus represented at a very early stage in the visual system.

Much less, however, is known about how the outputs of these first-stage cortical cells, or filters, are combined to give rise to the perception of textured surfaces. There are currently two different classes of models, and they are illustrated in figure 1. In one class of model, which we refer to here generically as the ‘feature model’, the stimulus is represented initially in terms of what are sometimes termed ‘primitives’. In Treisman’s (1985) classical model of pre-attentive vision, the primitive are features such as element orientation, spatial frequency, color, brightness, direction of movement, etc. These attributes are identified and coded into individual feature maps. The manner in which the visual system might identify features from a given image is typically not made explicit in feature models. After feature maps have been constructed, any differences within a given feature map, for example a horizontal line, or lines, amongst vertical lines, can be pre-attentively processed, resulting in ‘pop out’ or effortless texture segregation. Conjunctions of features, however, for example a line

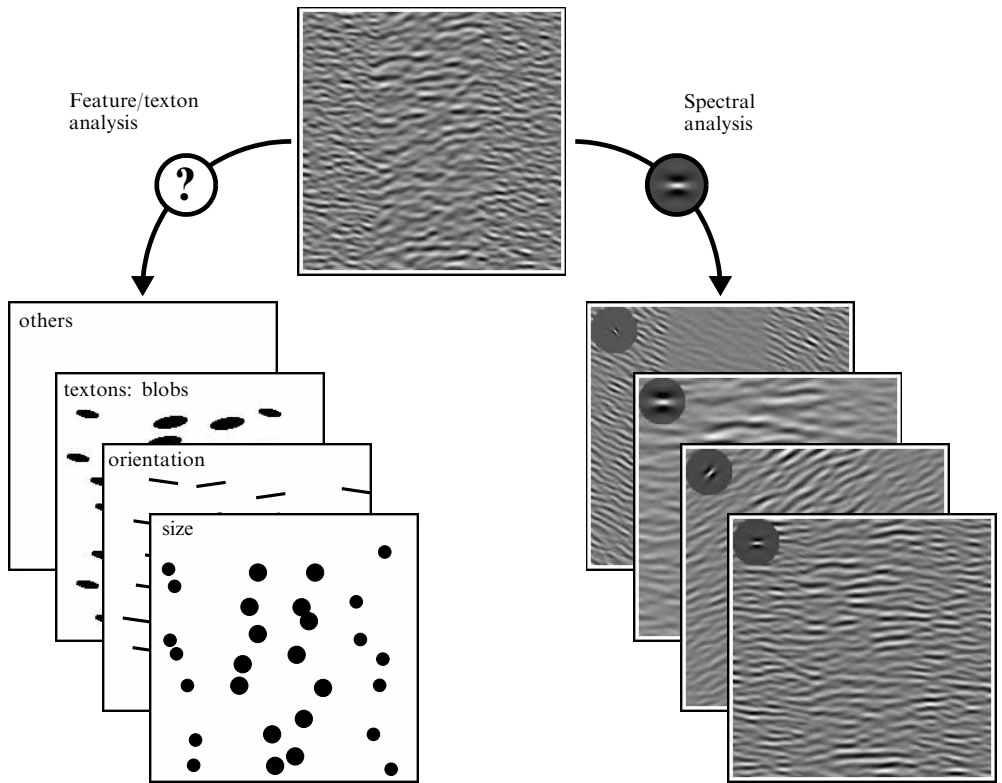


Figure 1. Schematic depictions of feature/texton-based mechanisms (left) and energy-based texture mechanisms (right). In the feature/texton-based approach, abstract representations of primitives are created in separate feature and texton maps. In the energy-based approach of texture segmentation, however, different maps correspond to the activation of channels of orientation-selective and spatial-frequency-selective filters.

that is both horizontal and large set amongst both small horizontal and large vertical lines, is more difficult to detect because it requires information to be combined across different feature maps (eg orientation and spatial frequency). This integration of information across feature maps requires allocation of limited-capacity attention. A large body of research has concentrated on exactly which visual attributes may be classified as features (see Wolfe 1998 for a comprehensive review).

Julesz and collaborators (Bergen and Julesz 1983; Julesz 1981; Julesz and Kröse 1988) have argued for primitives that are more complex than Treisman's features, and have termed them textons. Textons are descriptive abstractions such as elongated blobs, defined by a combination of orientation, length, width, and position, together with their terminators. Other textons are colors and line crossings. Accordingly, if two texture regions differ in the density of a given texton, they should effortlessly discriminate. The idea that the identification of feature-based primitives is a necessary precursor for subsequent stages in vision also finds expression in Marr's (1982) influential notion of the 'primal sketch'. Here, critical image features such as edge and bar segments are labeled locally according to their orientation, blur, contrast, color, etc, and the resulting description is then used for higher processing.

All these approaches share the common idea that some kind of explication of local feature content precedes the analysis of surface properties such as texture. What primitives are identified, as well as the manner in which these primitives are identified, however, remains largely a matter of conjecture.

The second class of model, referred to here as the ‘energy model’, proposes that texture modulations are detected by mechanisms that directly compare the responses of first-stage cortical filters (eg simple cells) between different texture regions (eg Graham and Sutter 1998; Graham and Wolfson 2004; Landy and Bergen 1991; Malik and Perona 1990). In order to compare the filter responses between different texture regions, it is necessary to prevent excitatory and inhibitory responses from canceling when pooled, and for this a nonlinearity such as rectification or squaring is necessary, resulting in the delivery of ‘energy’ responses. The ‘maps’ in this case are therefore of the energy responses of filters tuned to particular orientations and spatial frequencies (figure 1).

There has been a long-standing debate between proponents of Julesz’s texton-based theory of texture processing and proponents of the energy model. Typically, proponents of Julesz’s theory have argued that, because one can create textures which segment effortlessly yet whose global Fourier spectra are invariant across the texture border, the texton theory is supported (eg Bergen and Julesz 1983; Caelli and Julesz 1978; Julesz and Kröse 1988). However, proponents of the energy approach have shown that by incorporating relatively simple and physiologically plausible nonlinearities (such as the separation of ‘ON’ and ‘OFF’ filter responses followed by half-wave rectification) energy mechanisms can distinguish between such textures (eg Bergen and Adelson 1988; Malik and Perona 1990; Sagi 1994). Moreover, the existence of such textures does not constitute proof against the idea that at least some textures are processed by energy mechanisms.

The appeal of energy mechanisms has lain primarily in being founded on well-established cortical physiology (linear bandpass filters in area 18/V1), and in its computational simplicity. Although much research has focused on investigating properties of energy mechanisms, such as the nature of the nonlinearity following initial filtering of the visual scene (eg Chubb et al 1994; Graham and Sutter 1998), the relation between orientation preferences of the first-stage and second-stage filters (eg Graham and Wolfson 2001; Wolfson and Landy 1995), the temporal properties of energy mechanisms (eg Motoyoshi and Nishida 2001), etc, until now there has been little direct evidence in support of the energy approach per se. That is to say, little evidence exists that not only confirms predictions based on the energy approach but also contradicts predictions made by the feature-based approach. Bergen and Adelson (1988) created a texture which, despite containing texture regions differing in featural content, did not segment effortlessly. This finding directly contradicts the feature model. Adelson and Bergen also showed that an energy mechanism can be constructed which mirrors human’s inability to pre-attentively segment this texture. This demonstration indicates that an energy mechanism is at least consistent with human performance for this texture, whereas a feature model is not.

Here we provide direct evidence for the existence of an energy mechanism underlying the processing of texture modulations. We have utilized a rather curious and at first sight counterintuitive prediction of the energy mechanism. Because energy mechanisms detect differences in the responses of first-stage filters across space/time, it can be shown that the most responsive energy mechanism may receive first-stage inputs from channels that are ‘off-orientation’ and/or ‘off-frequency’, ie channels tuned to orientations and spatial frequencies that do not match those most prominently present in the stimulus.

In a previous study, we tested this prediction (Prins and Kingdom 2002). We used orientation-modulated (OM) textures such as shown in figure 2a. Such textures consist of a multitude of randomly positioned micropatterns, each with a specific orientation and spatial frequency. The textures were divided into several bar-shaped regions. In order to create an OM texture, alternating regions were filled with micropatterns which differed in orientation. For example, the texture in figure 2a consists of regions containing micropatterns tilted clockwise from horizontal by 20° alternated with regions containing micropatterns tilted counterclockwise from horizontal by 20°.

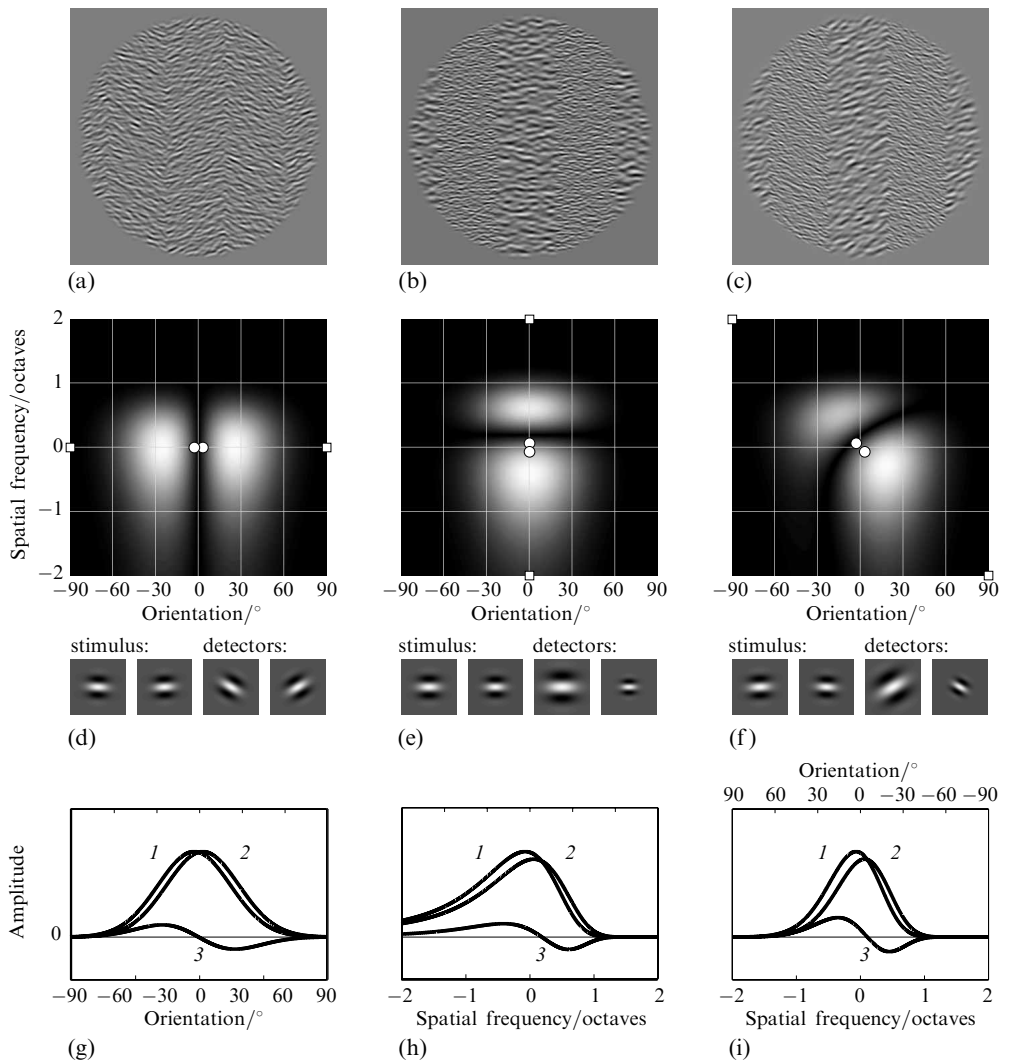


Figure 2. Example textures and difference spectra: (a) Example orientation-modulated (OM) texture. Modulation amplitude is 20° (peak-to-trough difference is 40°). (b) Example frequency-modulated (FM) texture. Modulation amplitude is 0.4 octaves. (c) Example conjoint-modulated texture. Orientation-modulation amplitude is 20° and frequency-modulation amplitude is 0.4 octaves. (d)–(f) Absolute differences between contrast spectra of the two regions of OM, FM, and conjoint-modulated textures, respectively, across orientations and spatial frequencies are shown in the panels as large, blurry white blobs. The modulation amplitudes in plots (d)–(f) are 3° and 0.067 octaves. These values are comparable to the detection thresholds of the observers. The small white circles correspond to the nominal peaks in orientation and spatial frequency of the texture regions. Note that the peaks in the difference distribution lie well outside the nominal peaks of the texture region. For example, for the OM texture the difference in contrast peaks at about 30° from horizontal. Also shown are micropatterns with orientation and spatial-frequency characteristics corresponding to the nominal peaks in the stimulus ('stimulus') as well as micropatterns with orientation and spatial-frequency characteristics corresponding to the peaks in the contrast-difference distribution (ie micropatterns that match the tuning of those filters predicted to be maximally tuned to detect the texture modulation, 'detectors'). (g)–(i) 1-D representations of the contrast distribution along the lines connecting the white squares in (d)–(f). Shown are the averaged contrast in the two texture regions making up each texture (1) and (2) as well as the difference between them (3).

However, as with any spatially finite element, the micropatterns contain contrast energy not only at their nominal peak orientation. Rather, the micropatterns contain contrast energy at a range of orientations and, as a result, will stimulate simple-cell-like detectors tuned to a wide range of orientations. Figures 2d and 2g show the differences in contrast energy across orientations and spatial frequencies between the two different texture regions of an OM texture at a modulation amplitude of 3° (ie texture regions containing micropatterns tilted 3° clockwise from horizontal are alternated with texture regions containing micropatterns tilted 3° counterclockwise from horizontal; this value is similar to the detection threshold for the observers). Whereas the small white circles in figure 2d correspond to the nominal peak orientations and spatial frequencies in the two regions, the large white blobs correspond to the (absolute) difference in contrast energy between the two regions across orientations and spatial frequencies. Below each plot are shown micropatterns with orientation and spatial-frequency characteristics corresponding to the nominal peaks in the stimulus ('stimulus') as well as micropatterns with orientation and spatial-frequency characteristics corresponding to the peaks in the contrast-difference distribution. The latter micropatterns are labeled 'detectors' in the figure since first-stage filters with these orientation and spatial-frequency tunings would lead to the biggest differential response between the two texture regions. Two things should be noted. First, the two texture regions contain approximately equal contrast energy at the peak orientation of either texture region. Second, the two texture regions differ most at 'off-orientations' centered at about 30° in either direction from horizontal. Using a psychophysical adaptation paradigm that will be described below, we found evidence that OM textures are indeed processed by channels tuned to 'off-orientations' (Prins and Kingdom 2002).

We also tested whether frequency-modulated (FM) textures are processed by 'off-frequency' channels. Figure 2b shows an example FM texture, in which the two different texture regions differ in spatial frequency by 0.8 octaves. Figures 2e and 2h show the differences in energy across orientations and spatial frequencies between the two different texture regions of an FM texture at a modulation amplitude of 0.067 octaves (a value which is similar to the detection threshold for the observers). As the figure shows, the two regions of an FM texture differ most prominently at 'off-frequencies' centered at about 0.5 octaves above and below the nominal peak frequencies of the two regions. We confirmed that FM textures are processed by channels tuned to 'off-frequencies' (Prins and Kingdom 2002).

These results thus confirm the most distinctive characteristic of the energy model, which is that energy models directly process the existing differences between texture regions. This finding is not, however, necessarily inconsistent with a feature-based approach. As we have mentioned above, feature models are typically not explicit how features are identified. It is possible that the nominal or peak orientation is identified through off-orientation simple cells (eg Regan and Beverley 1985), for example on the basis of the extreme values in the first derivative of the population activity across different orientations. Likewise, the nominal or peak spatial frequency might be identified through off-spatial-frequency simple cells (eg Regan and Beverley 1983). It is thus possible to derive an orientation map and a spatial-frequency map utilizing the information from these channels of 'off-peak' simple cells. The results of Prins and Kingdom (2002) are thus compatible with at least this specific implementation of the feature model.

In the present research, we utilize textures that are modulated in both orientation and frequency, as in the 'conjoint-modulation' example in figure 2c. For such conjoint modulations, the predictions for the energy model are not compatible with feature models.

The energy model, as before, predicts that conjoint textures are detected by channels that are tuned to the differences between the two texture regions. The peak differences between the texture regions lie at locations in orientation/frequency space that are determined by the specific combination of modulation amplitudes. For example, in figures 2f and 2i are shown the differences in contrast energy between the two texture regions when the orientation and frequency modulations are combined such that clockwise tilted micropatterns are of higher frequency than counterclockwise tilted micropatterns. The small white circles in figure 2f again correspond to the nominal peak orientation and spatial frequency of the two different texture regions (values were chosen that were comparable to threshold modulation amplitudes for the observers). Feature-based models make no specific predictions as to the luminance channels involved in the construction of feature maps. However, we will argue in section 4 that the predictions of the energy model are not compatible with feature-based models in that they contradict a number of fundamental tenets of feature-based models of texture processing.

Here we use the same technique as that described by us earlier (Prins and Kingdom 2002). Our observers were to determine whether conjoint-modulated textures contained four or eight texture bars. However, before testing, observers adapted to a luminance grating of a specific orientation and spatial frequency. We measured the threshold modulation amplitudes as a function of the orientation and spatial frequency of the adapting grating. The adaptation selectively desensitized the channels responsive to the orientation and spatial frequency of the adapting grating. When a channel relevant to the task is desensitized, the threshold amplitude of modulation is expected to increase. Hence, this technique allows us to determine which first-order channels are involved in the detection of the texture modulation.

2 Method

2.1 Stimuli

Stimuli consisted of circular textures (radius 4.2 deg). Example stimuli are shown in figure 3. The textures were constructed by randomly positioning a multitude of Gabor-shaped micropatterns within the stimulus area.

The micropatterns were described by:

$$L(x, y) = L_0 + L_m \cos[2\pi f(x \sin \theta + y \cos \theta) + \varphi] \exp\left(-\frac{x^2 + y^2}{2\sigma_e^2}\right) \quad (1a)$$

where

$$\sigma_e = \frac{(0.5 \ln 2)^{1/2} (2^{\text{BW}} + 1)}{f\pi(2^{\text{BW}} - 1)}, \quad (1b)$$

$L(x, y)$ is luminance as a function of spatial position (x, y) , L_0 is mean luminance (124.0 cd m^{-2}), L_m is the luminance modulation amplitude (61.9 cd m^{-2}), f is spatial frequency, θ is orientation (horizontal = 0° ; increasing θ corresponds to counterclockwise rotation), φ is the phase of the cosine component ($\varphi = \pi/2$ or $3\pi/2$), σ_e is the standard deviation of the Gaussian envelope, and BW is the spatial-frequency bandwidth of the micropatterns, which was set to 1.5 octaves. The value of σ_e covaried with the value of f so as to keep the spatial-frequency bandwidth (full-width at half-height) of the micropatterns constant at 1.5 octaves across different frequencies. In order to avoid excessive luminance summation, the center-to-center distance between any two micropatterns was constrained to equal at least the standard deviation of the contrast envelope of the micropattern [σ_e in formula (1b)]. In order to ensure equal rms contrast between regions of differing spatial frequency, the density of Gabor micropatterns was varied with f such that the number of micropatterns per $(1 \text{ deg})^2$ was $0.6/\sigma_e^2$.

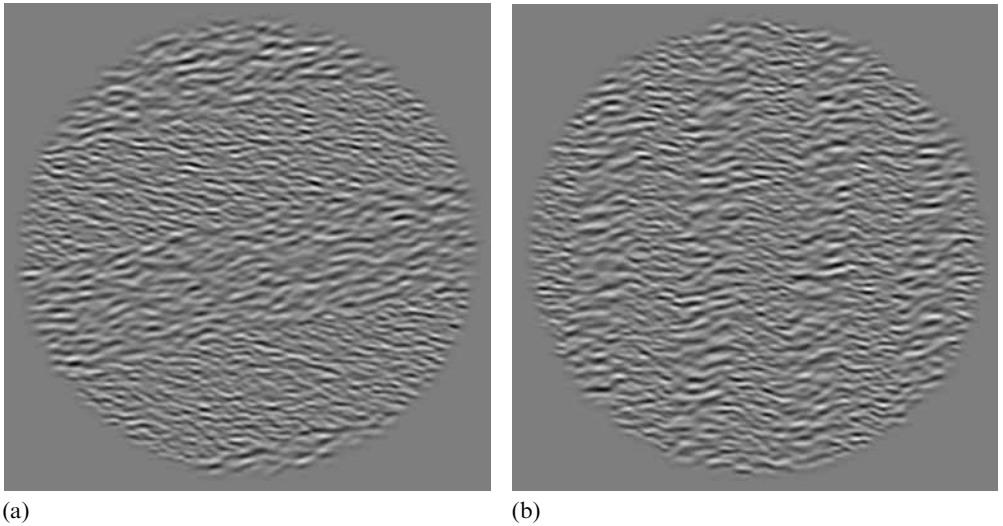


Figure 3. Example conjoint-modulated textures: (a) texture containing four texture bars; (b) texture containing eight texture bars. Amplitude of orientation modulation is 8° , amplitude of spatial-frequency modulation is 0.2 octaves (these values correspond roughly to three times NP's threshold).

Textures thus constructed contain a range of orientations and spatial frequencies that is well-described by a relatively simple mathematical formula. The average contrast of the texture regions across orientation (θ) and spatial frequency (f) is proportional to:

$$\frac{1}{f_0} \exp \left[-0.5 \left(\frac{f - f_0}{0.41 f_0} \right)^2 \right] \exp \left[-0.5 \left(\frac{\theta - \theta_0}{25.5} \right)^2 \right],$$

where f_0 and θ_0 are the center spatial frequency and orientation of the texture region, respectively (Prins and Kingdom 2002).

For the main experimental manipulation, the center orientation and spatial frequency of the micropatterns were jointly square-wave modulated. In other words, the textures were subdivided into bars of equal width which consisted alternately of high-frequency micropatterns tilted clockwise from horizontal and low-frequency micropatterns tilted counterclockwise from horizontal. The spatial frequency of the micropatterns [f in formula (1a)] was modulated relative to a center spatial frequency of 5 cycles deg^{-1} such that the spatial frequencies in the two texture regions differed from this center spatial frequency by an equal number of logarithmic frequency units. The orientation of micropatterns [θ in formula (1a)] was modulated around horizontal. The relative amplitude of modulation of the two components (orientation and spatial frequency) was such that they were presented at equal proportions of their individual thresholds obtained when the components were modulated separately. These thresholds were determined for observers individually before the main experiment.

The width of the texture bars was varied such that the texture contained either four or eight bars. The phase and orientation of the texture modulation was varied randomly from trial to trial.

Textures were generated online and presented on a Clinton Monoray monitor driven by a Cambridge Research Systems VSG2/5. At the employed viewing distance of 100 cm, the resolution of the monitor was 42.3 pixels deg^{-1} .

2.2 Subjects

Both authors served as observers. Observers had normal or corrected-to-normal vision.

2.3 Procedure

At the start of each session, observers adapted to a simple sine luminance grating presented at 63% contrast for 120 s. The adapting grating was presented in a square region ($9.1 \text{ deg} \times 9.1 \text{ deg}$) which was centered on the stimulus region. The adapting grating reversed contrast at a rate of 1 contrast-reversal s^{-1} . After initial adaptation the following sequence was repeated: blank screen (250 ms), test stimulus (250 ms), blank screen (250 ms), adapting grating (6 s). The adapting grating again reversed contrast at a rate of 1 contrast-reversal s^{-1} . Observers were to indicate whether the texture contained four or eight texture bars. Reaction times were not recorded but observers were required to respond within 3250 ms after stimulus offset, at which point feedback was given in the form of a tone following an incorrect response. The amplitude of modulation was varied from trial to trial by an adaptive staircase procedure (the best PEST—Pentland 1980). Three independent staircases of 40 trials each were randomly interleaved for a total of 120 trials per session. Thresholds for the unadapted conditions were obtained as above, except that the contrast of the adapting grating was set to zero.

3 Results

Within each condition, responses were combined across the different staircases and fitted with a logistic function using a maximum-likelihood criterion. Standard errors of the thresholds (at 75% correct) were determined by bootstrap analysis with 400 repetitions for each standard error (eg Efron and Tibshirani 1986). Modulation amplitudes are expressed as half the peak-to-trough difference in orientation and spatial frequency between the two different texture regions.

In table 1, we list the thresholds for individual OM and FM modulations as well as the thresholds for the conjoint modulation. All these thresholds were measured without adaptation.

Table 1. Thresholds and standard errors for orientation-modulated, frequency-modulated, and conjoint-modulated textures. Standard errors are listed in parentheses. Thresholds were obtained without adaptation.

Observer	Type of modulation		
	Orientation/ $^{\circ}$	Frequency/octaves	Conjoint/ $^{\circ}$, octaves
NP	2.82 (± 0.18)	0.069 (± 0.003)	2.05 (± 0.09), 0.050 (± 0.002)
FK	2.96 (± 0.13)	0.077 (± 0.005)	2.08 (± 0.11), 0.054 (± 0.003)

Threshold elevations (adapted versus unadapted threshold ratios) for the adapted conjoint-modulation conditions and their standard errors are shown in figure 4 as a function of the spatial frequency (SF) and orientation of the adapting grating. Results of both observers confirm the critical predictions of the energy model. First, adaptation to a grating with orientation and spatial frequency close to the dominant orientation and spatial frequency of the texture [middle panel, 'SF = dc (5 cycles deg^{-1} ') and orientation = 0°] has little, if any, effect on thresholds. Instead, threshold elevations peak at 'off-orientations' and 'off-frequencies'. More importantly, threshold elevations peak at specific combinations of orientations and spatial frequencies of the adapting grating. Whereas low-frequency adaptors elevate thresholds maximally when they are tilted counterclockwise (eg when SF = -0.5 octaves, threshold elevations peak around $+30^{\circ}$), high-frequency adaptors elevate thresholds maximally when they are tilted clockwise (eg when SF = $+0.5$ octaves, threshold elevations peak around -30°).

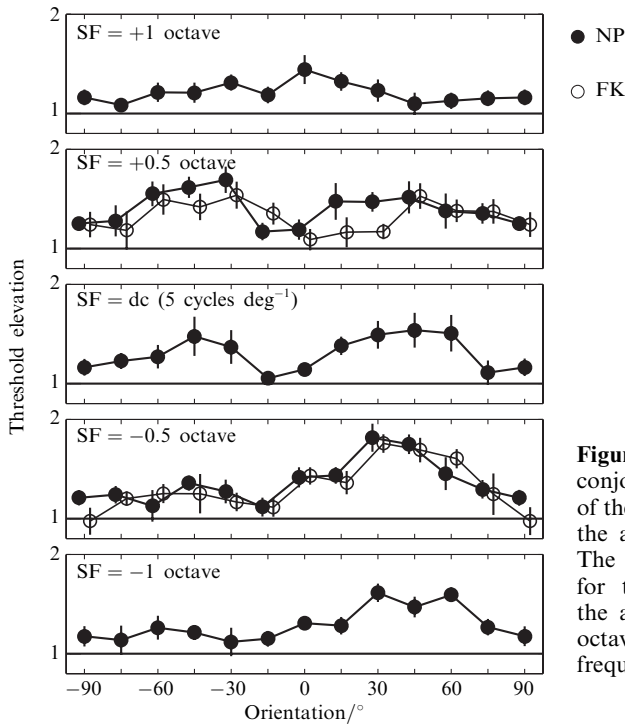


Figure 4. Threshold elevations for the conjoint-modulated textures as a function of the orientation and spatial frequency of the adapting grating for both observers. The different panels show the results for the different spatial frequencies of the adapting grating which are given in octaves relative to the texture ‘dc’ spatial frequency ($5 \text{ cycles deg}^{-1}$).

These effects are visible more clearly in figure 5, where NP’s threshold elevations are plotted as a contour plot in orientation/spatial-frequency space, for easy comparison with the predictions of the energy model presented in figure 2f. It is clear from figure 5 that threshold elevations peak in two distinct clusters, centered around adaptors which are both off-orientation and off-frequency.

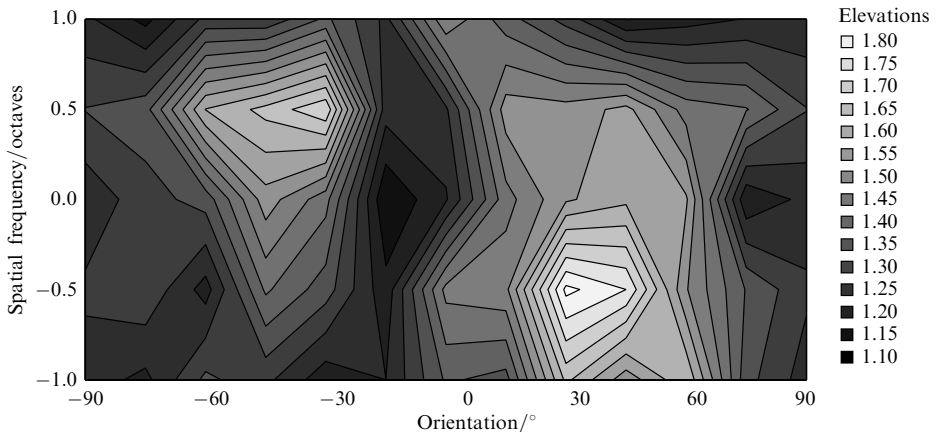


Figure 5. Observer NP’s pattern of threshold elevation plotted as a contour.

4 Discussion

We have shown before (Prins and Kingdom 2002) that individual OM and FM modulations in textures are processed by mechanisms that are optimized to detect contrast differences across space within narrow orientation and spatial-frequency bands. Here we show that conjoint-modulated textures are processed in the same manner. Threshold elevations peaked when observers were adapted to gratings of those orientations and

spatial frequencies at which the two texture regions differed most in the energy contained in them. These specific orientations and spatial frequencies are determined by the specific combination of orientation and spatial-frequency amplitudes of our conjoint modulations.

As mentioned in section 1, feature models typically make no explicit statements how features might be identified from an image. As such, feature models make no specific predictions which first-order channels might be involved in the processing of textures such as ours. However, three critical characteristics of feature models are contradicted by our results. First, according to the feature model, differences in featural content between texture regions are detected only after feature maps are created. Construction of the feature maps could therefore not possibly be guided by, or depend on, the existing differences between texture regions. Rather, it should depend exclusively on the characteristics of the individual texture regions. Yet it is clear that the tunings of the channels involved in the processing of our textures do depend critically on the differences between the texture regions and are not directly related to the orientation and spatial-frequency content of the individual texture regions themselves.

Second, the feature model holds that the feature maps for orientation and spatial frequency, being two separate features, should each be constructed independently. Our results are inconsistent with this idea. If the orientation and spatial-frequency modulations were processed separately, one would expect that the pattern of threshold elevations as a function of the orientation and spatial frequency of the adapting grating would be some linear combination of the patterns found for individual OM and individual FM modulations. That is, one would expect to find threshold elevations at four distinct orientation/spatial-frequency combinations: two of these would correspond to the predicted pattern for OM textures (figure 2d), two more would correspond to the predicted pattern for FM textures (figure 2e). Our pattern of results, however, consists of two distinct peaks in orientation/spatial-frequency space that cannot be derived as a linear combination of those predicted for individual OM and FM modulations.

Finally, a fundamental tenet of the feature model is that texture segregation is based on a comparison of the featural content between texture regions. However, the featural content of texture regions cannot be established by determining contrast differences in the channels we have shown to be involved. On the basis of the activation of these channels it is not possible to determine either the dominant orientation or the dominant spatial frequency in our texture regions. For example, it is possible to create texture modulations that show the same pattern of contrast differences across orientations and spatial frequencies as our textures do but that do not contain any energy at the horizontal orientation or the dominant spatial frequency of our textures.

Our results thus provide the first direct evidence for the existence of an energy mechanism. That is, we have confirmed that texture modulations are processed by comparing contrast within relatively narrow orientation and spatial-frequency bands across space, and we have shown that our results can not be explained by a feature model.

It is important to note that we have not disproven the existence of feature-based or texon-based mechanisms. As a matter of fact, a vast body of evidence indicates that different featural attributes of objects are, at some level of processing, represented disjointly in the visual system. For example, when two differently colored characters are briefly presented, observers may mismatch the colors and identities of the characters (eg Treisman and Schmidt 1982). There is an obvious benefit to creating explicit featural representations of the visual scene and observers are indeed highly accurate at determining, for example, the dominant orientation of a texture. Energy-based texture mechanisms are unable to create such a representation. Energy-based texture mechanisms only carry information regarding the differences in energy between texture regions within narrow orientation/spatial-frequency channels and do not carry any

information regarding the predominant featural content of the texture. As such, energy mechanisms continue the trend of earlier visual neurons to code relative, rather than absolute, image properties. Compare an energy mechanism, for example, with geniculate center-surround cells which code only for relative brightness and carry no information regarding absolute brightness.

Finally, it is interesting to note that energy mechanisms also do not carry information regarding the nature of the image property that is being modulated. For example, from the activation of any particular energy mechanism it cannot be determined that the texture contains, say, an orientation modulation rather than a frequency modulation (but see Prins and Kingdom 2003).

Acknowledgments. This research was supported by a grant from the Natural Sciences and Engineering Research Council of Canada (NSERC) Grant OGP 0121713. We are grateful for many insightful comments made by anonymous reviewers.

References

- Bergen J R, Adelson E H, 1988 "Early vision and texture perception" *Nature* **333** 363–364
- Bergen J R, Julesz B, 1983 "Parallel versus serial processing in rapid pattern discrimination" *Nature* **303** 696–698
- Caelli T, Julesz B, 1978 "On perceptual analyzers underlying visual texture discrimination: Part I" *Biological Cybernetics* **28** 167–175
- Campbell F W, Cooper G F, Enroth-Cugell C, 1969 "The spatial selectivity of the visual cells of the cat" *Journal of Physiology* **203** 223–235
- Chubb C, Econopouly J, Landy M S, 1994 "Histogram contrast analysis and the visual segregation of IID textures" *Journal of the Optical Society of America A* **11** 2350–2374
- Cutting J E, Millard R T, 1984 "Three gradients and the perception of flat and curved surfaces" *Journal of Experimental Psychology: General* **113** 198–216
- Efron B, Tibshirani R, 1986 "Bootstrap methods for standard errors, confidence intervals, and other measures of statistical accuracy" *Statistical Science* **1** 54–75
- Frisby J P, Buckley D, 1992 "Experiments on stereo and texture cue combination in human vision using quasi-natural viewing", in *Artificial and Biological Visual Systems* Ed. H H Orban (Berlin: Springer) pp 267–297
- Graham N, Sutter A, 1998 "Spatial summation in simple (Fourier) and complex (non-Fourier) texture channels" *Vision Research* **38** 231–257
- Graham N, Wolfson S S, 2001 "A note about preferred orientations at the first and second stages of complex (second-order) texture channels" *Journal of the Optical Society of America A* **18** 2273–2281
- Graham N, Wolfson S S, 2004 "Is there opponent-orientation coding in the second-order channels of pattern vision?" *Vision Research* **44** 3145–3175
- Hubel D H, Wiesel T N, 1962 "Receptive fields, binocular interaction and functional architecture in the cat's visual cortex" *Journal of Physiology* **160** 106–154
- Julesz B, 1981 "Textons, the elements of texture perception, and their interactions" *Nature* **290** 91–97
- Julesz B, Kröse B, 1988 "Features and spatial filters" *Nature* **333** 302–303
- Knill D C, 1998 "Discrimination of planar surface slant from texture: human and ideal observers compared" *Vision Research* **38** 1683–1711
- Knill D C, 2001 "Contour into texture: information content of surface contours and texture flow" *Journal of the Optical Society of America A* **18** 12–35
- Landy M S, Bergen J R, 1991 "Texture segregation and orientation gradient" *Vision Research* **31** 679–691
- Li A, Zaidi Q, 2000 "Perception of three-dimensional shape from texture is based on patterns of oriented energy" *Vision Research* **40** 217–242
- Malik J, Perona P, 1990 "Preattentive texture discrimination with early vision mechanisms" *Journal of the Optical Society of America A* **7** 923–932
- Marr D, 1982 *Vision: A Computational Investigation into the Human Representation and Processing of Visual Information* (San Francisco, CA: W H Freeman)
- Motoyoshi I, Nishida S, 2001 "Temporal resolution of orientation-based texture segregation" *Vision Research* **41** 2089–2105
- Pentland A, 1980 "Maximum likelihood estimation: the best PEST" *Perception & Psychophysics* **28** 377–379

-
- Prins N, Kingdom F A A, 2002 "Orientation- and frequency-modulated textures at low depths of modulation are processed by off-orientation and off-frequency texture mechanisms" *Vision Research* **42** 705–713
- Prins N, Kingdom F A A, 2003 "Detection and discrimination of texture modulations defined by orientation, spatial frequency, and contrast" *Journal of the Optical Society of America A* **20** 401–410
- Regan D, Beverley K I, 1983 "Spatial frequency discrimination and detection: comparison of postadaptation thresholds" *Journal of the Optical Society of America* **73** 1684–1690
- Regan D, Beverley K I, 1985 "Postadaptation orientation discrimination" *Journal of the Optical Society of America A* **2** 147–155
- Sagi D, 1994 "The psychophysics of texture segmentation", in *Early Vision and Beyond* Ed. T V Pappathomas (Cambridge, MA: MIT Press) pp 69–78
- Treisman A, 1985 "Preattentive processing in vision" *Computer Vision, Graphics, and Image Processing* **31** 156–177
- Treisman A, Schmidt H, 1982 "Illusory conjunctions in the perception of objects" *Cognitive Psychology* **14** 107–141
- Wolfe J M, 1998 "Visual search", in *Visual Attention* Ed. H Pashler (London: University College London Press) pp 13–71
- Wolfson S S, Landy M S, 1995 "Discrimination of orientation-defined texture edges" *Vision Research* **35** 2863–2877

ISSN 0301-0066 (print)

ISSN 1468-4233 (electronic)

PERCEPTION

VOLUME 35 2006

www.perceptionweb.com

Conditions of use. This article may be downloaded from the Perception website for personal research by members of subscribing organisations. Authors are entitled to distribute their own article (in printed form or by e-mail) to up to 50 people. This PDF may not be placed on any website (or other online distribution system) without permission of the publisher.